Article

Optical Coherence Tomography (OCT) for Time-Resolved Imaging of Alveolar Dynamics in Mechanically Ventilated Rats

Christian Schnabel [1,*], Maria Gaertner [1,2] and Edmund Koch [1]

[1] Department of Anesthesiology and Intensive Care Medicine, Clinical Sensoring and Monitoring, Faculty of Medicine CGC, Technische Universität Dresden, Dresden 01307, Germany; maria.gaertner@me.com (M.G.); edmund.koch@tu-dresden.de (E.K.)

[2] InfraTec GmbH, Gostritzer Straße 61-63, Dresden 01217, Germany

[*] Correspondence: christian.schnabel@tu-dresden.de; Tel.: +49-351-458-6133

Abstract: Though artificial ventilation is an essential life-saving treatment, the mechanical behavior of lung tissue at the alveolar level is still unknown. Therefore, we need to understand the tissue response during artificial ventilation at this microscale in order to develop new and more protective ventilation methods. Optical coherence tomography (OCT) combined with intravital microscopy (IVM) is a promising tool for visualizing lung tissue dynamics with a high spatial and temporal resolution in uninterruptedly ventilated rats. We present a measurement setup using a custom-made animal ventilator and a gating technique for data acquisition of time-resolved sequences.

Keywords: optical coherence tomography; OCT; mechanical ventilation; lung imaging

1. Introduction

Lung diseases and related affections of the body are one of the most common diseases in the industrial world [1]. Therefore, suitable treatment strategies are necessary using protective mechanical ventilation that shows a significant reduction in morbidity and mortality of affected patients [2,3]. Beside this effort, a detailed understanding of the mechanical transactions in alveolar lung tissue is still lacking. Hence, the choice of appropriated ventilation strategies and parameters during mechanical ventilation is essential to avoiding vast damage in sensitive alveolar tissue and to assure a patient's treatment success. A proper decision should be based on the detailed knowledge of tissue behavior during ventilation with respect to the particular disease. Common imaging techniques such as CT or MRT used in human diagnostics are not appropriate for investigating the ventilation effects on the microscale of alveoli. Therefore, it is of great medical and scientific interest how mechanical ventilation affects lung tissue on the alveolar level of gas exchange. Detailed insights into lung tissue behavior can be achieved in animal experiments using high-resolution imaging methods such as optical coherence tomography (OCT). In combination with intravital microscopy (IVM), both imaging techniques allow for the visualization of alveolar structures with a high spatial resolution [4,5]. Further information can be gathered investigating the tissue dynamics. This challenging task is commonly solved by high-speed OCT systems using Fourier-domain mode locked lasers [6] with the disadvantage of either a small scan area or a bad spatial resolution. Therefore, in the presented study, we used a custom-made ventilator and a new gating algorithm for image data acquisition to get new insights into lung tissue behavior on the alveolar level during uninterrupted mechanical ventilation in rats. These measurements can promote the understanding of alveolar mechanics and the effort for the development of more protective ventilation strategies.

2. Materials and Methods

2.1. Imaging Setup

The imaging system used for the investigation of lung tissue dynamics during ventilation is a combination of OCT and IVM using the same beam path in one scanner head. The custom-made OCT setup is described in detail by Meissner et al. [7]. Shortly, the system consists of a superluminescence diode (Superlum, Moscow, Russia) centered at 845 nm with a FWHM of 50 nm. As OCT is based on the use of a Michelson interferometer, the emitted near-infrared light is separated into a reference beam and a sample beam. The sample beam is deflected using two galvanometer scanners (Cambridge Technology Inc., Cambridge, MA, USA) to perform a 2D-scan pattern (x and y) over the sample. The scattered and reflected light from different sample depths (z) is collected and superimposed with the reference beam that was reflected on a mirror. This interference signal is spectrally resolved by a diffraction grating and measured by a line-detector (Teledyne DALSA Inc., Bromont, QC, Canada). The depth-dependent information is calculated by a Fast Fourier Transformation of the spectrum and results in a depth profile of backscattered light called an A-scan. Displaying the logarithm of the intensity from several A-scans at different transversal positions on an 8 bit grayscale results in a cross-sectional view called a B-scan. The axial and lateral resolution are 11 μm and 6 μm in air, respectively. The line scan rate is 12 kHz, which allows data acquisition of typical cross sections within 29 ms (320×512 pixels corresponding in this system to 1.28×2.8 mm (width $\times$ depth)).

For IVM, a high-speed video camera (acA2000-340 kc, Basler, Ahrensburg, Germany) in combination with an adjustable liquid lens (EL-10-30, Optotune AG, Dietikon, Swizerland) is used to acquire 2D surface images with a maximum framerate of 340 fps (frames per second) at a full resolution of 2040×1088 pixels, which corresponds to a field of view of 3×1.5 mm using a four-fold magnification (refer to Figure 1). Therefore, the IVM beam path is coupled into the same beam path used for OCT by a dichroic mirror. Illumination for IVM is achieved by using a custom-made white light LED ring at the bottom of the scanner head. The electrical lens is driven by a 20 kHz pulse width modulated current signal allowing a focal shift of 5 mm within a 15 ms response time. This effectively reduces the video image acquisition down to a maximum of 66 fps.

2.2. Image Acquisition and Data Processing

The focal plane of IVM was adjusted during artificial ventilation by tracking the pleural surface using the depth information from OCT cross sections. Previous experiments with our animal model have shown that lung tissue movement in the axial (z-) direction is limited to a maximum of 1 mm. Using conventional ventilation settings (especially avoiding high inspiration pressure) in addition to the physiological conditions of the thorax after surgery (refer to Section 2.3), the axial shift of the lung tissue is typically 0.6 mm. In OCT cross sections, the signal-to-noise ratio (SNR) is reduced with increasing depth (so-called "roll-off"). In former studies, the roll-off of our system was measured with 8 dB over 1.7 mm depth with an overall SNR of 87 dB. It means that an axial lung tissue movement smaller than 1 mm has just minor effect on OCT image quality and vice versa that the whole tissue movement can be visualized in the OCT cross sections (overall imaging depth 2.8 mm) without the need of refocusing. Therefore, the size of the OCT cross sections is reduced to 64×512 pixels (width $\times$ depth) leading to 8 ms per B-scan (125 B-scans per second). With this high temporal resolution for visualizing tissue movement, the OCT signal can be used to keep the lung in focus for IVM. Hence, the maximum intensity index, which always corresponds to the lung surface (brightest reflection at air-tissue interface), is extracted from two successive OCT cross sections and the difference of the index position in depth is calculated. Using a lens calibration curve obtained from preliminary tests, the new lens current is set to match the new focus position to grab the IVM image. Because one breath cycle is sufficient for an IVM recording, these video sequences were taken prior to the OCT data acquisition and saved as a video file.
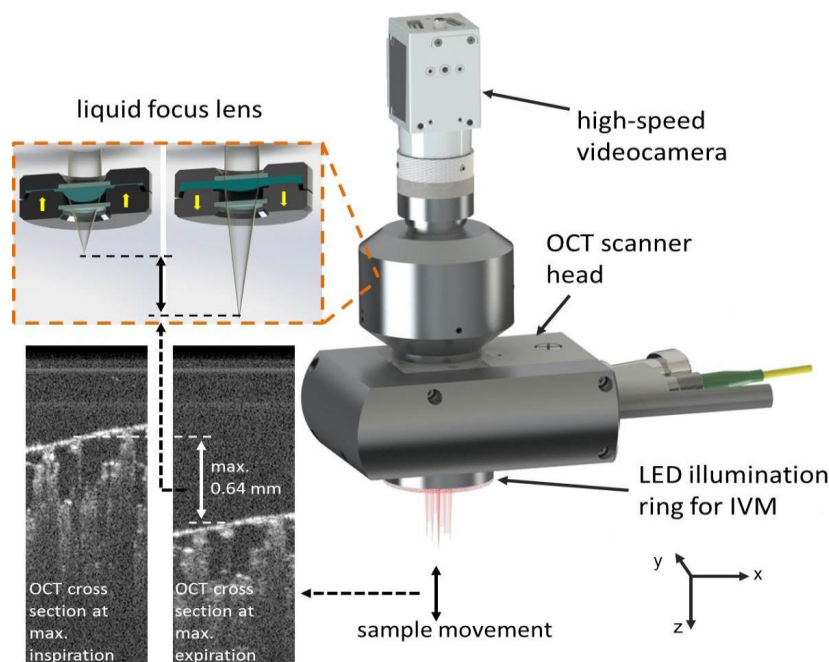
Figure 1. Scanner head for combined image acquisition with optical coherence tomography (OCT) and intravital microscopy (IVM). The adjustment of the focal plane for IVM is achieved by using a current driven liquid lens. The control signal to track the lung surface is generated by calculating the axial shift (in the *z*-direction) from successive OCT cross sections with a time gap in between of 8 ms (OCT image size of 64 × 512 pixels). The two exemplary OCT cross sections show a lung tissue at max. inspiration and max. expiration. The difference of lung surface in the *z*-direction between these two B-scans allows for the estimation of maximal lung movement, which was 0.64 mm in the data shown in this paper and up to 1 mm in former studies (not shown here). Both imaging techniques use the same beam path and show the same region of interest. Illumination for IVM is performed by using a LED ring.

Three-dimensional OCT data were acquired using two galvanometer scanners mounted perpendicularly to each other. For one single cross section, the first scanner deflects the light in one direction to measure several A-scans forming the OCT B-scan. Adjacent B-scans were recorded by tilting the second scanner, resulting in a three-dimensional image stack. As mentioned before, the line scan rate of this system is fixed to 12 kHz, resulting in 29 ms for a single cross section (320 × 512 pixels) and an overall measurement time of 9.2 s for an 3D image stack (320 × 320 × 512 pixels). As this takes much longer than a ventilation cycle in rats, other ways to acquire 3D image stacks are needed. Because the ventilation is periodic and changes in the viscoelastic properties of the lung are rather slow, we collected image data over a longer time period and rearranged the image data afterwards. Therefore, during one ventilation cycle, B-scans were acquired at the same line showing the axial tissue movement in one plane with a temporal resolution of 29 ms (using an image size of 320 × 512 pixels). That means that 34 cross sections can be acquired within a ventilation cycle time of 1 s (at an exemplary ventilation rate of 60 breaths per minute). After each ventilation cycle, a trigger signal from the ventilator sets the second scanner to the next position, and cross sections are grabbed continuously at this new position. Each acquired B-scan within a ventilation cycle is consecutively numbered and additionally marked by the corresponding cycle number. In a post-processing step, shown as scheme in Figure 2, all B-scans are re-sorted by using the index number and the trigger number to form the different 3D OCT stacks, each showing a different phase of the ventilation cycle. The general reconstruction is shown in Figure 2 where the rearrangement of OCT cross sections from successive ventilation cycles for the first 3D stack at the beginning of inspiration and the 14th OCT stack at maximum pressure are visualized (inspiration to expiration ratio I:E = 1:1 see below). The overall

amount of 3D stacks is 34 with a time gap in between of 29 ms corresponding to the acquisition time for one single B-scan. All 3D stacks are combined to the resulting 4D OCT stack, which shows the complete tissue movement during one breath although measured over several consecutive ventilation cycles. As a consequence of this procedure, the number of volume data per cycle can be increased either by decreasing the ventilation rate or by decreasing the size of the B-scans.
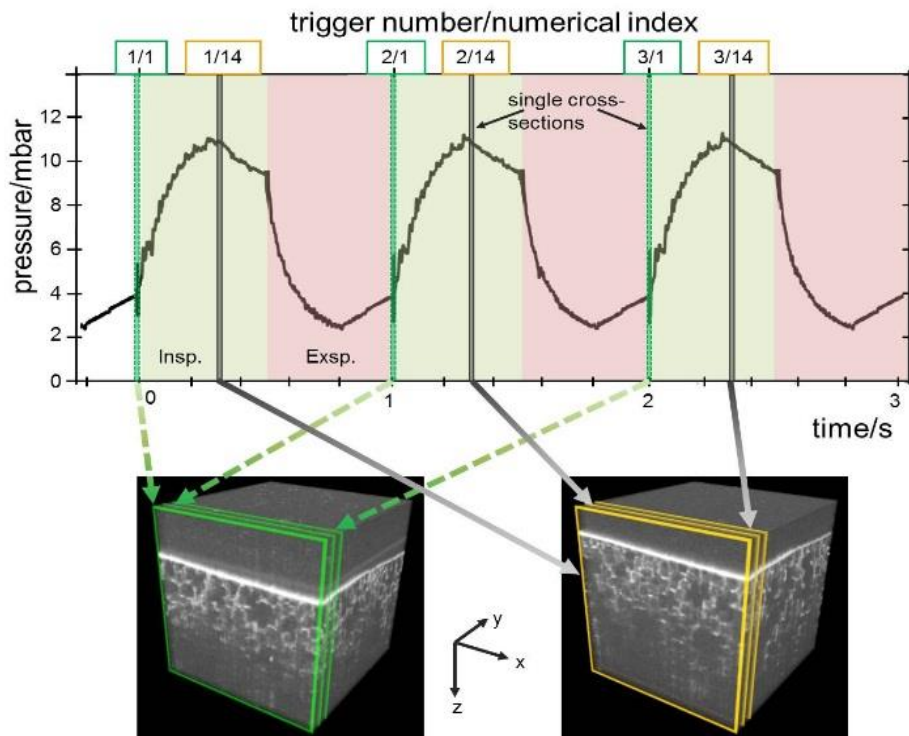

Figure 2. Example of 3D image reconstruction after measurement during uninterrupted artificial ventilation using the numerical index and the corresponding trigger number. Inspiration (light green) to expiration (light red) time ratio was 1:1. Each reconstructed 3D OCT stack shows a different phase of the tissue movement within the ventilation cycle. This procedure is shown in this figure for the first and the 14th 3D stack. Each first B-scan (marked by the numerical index 1) of the consecutive ventilation cycle (marked by the increasing trigger number) is rearranged to form the first 3D stack showing the tissue state at the beginning of the ventilation cycle. The 14th B-scan of each cycle is rearranged to form the 14th 3D stack showing the tissue at maximum pressure.

2.3. Animal Preparation and Artificial Ventilation

All experiments were approved by the animal care and use committee of the local government authorities (Landesdirektion Sachsen; AZ 24-9168.11-1/2012-17) and were performed in accordance with the Guide for Care and Use of Laboratory Animals (Institute of Laboratory Animal Resources, 7th edition, 1996). An in vivo rat model was used for imaging subpleural alveoli. Therefore, female rats (Sprague-Daley, 300 g) were anesthetized to a level at which spontaneous breathing effort is suppressed, intubated with a tracheal tube, and ventilated with 60 breaths per minute in a pressure-controlled manner from 2 to 11 mbar end-expiratory and end-inspiratory pressure, respectively. This deep anesthesia also helps to prevent disturbances in image acquisition. Nevertheless, plateau pressure controlled by servo loop and lung tissue response on overpressure ventilation can vary from cycle to cycle, resulting in small variations of tissue position. Optical access to the lung tissue is necessary for visualizing alveolar structures with OCT and IVM. Therefore, skin and muscle tissue between two ribs was removed by keeping the pleura visceralis intact to maintain the physiological thoracic pressure conditions. This procedure enabled a field of view of about 10×5 mm.

Artificial ventilation was performed by a custom-made ventilator described in detail by Schnabel et al. [5]. It consists of two independent custom-made syringe pumps and four magnetic valves to control flow direction. The user interface allows online interactions and a change of ventilator settings. It also provides measured parameters such as ventilated pressure and volume. A 5 V TTL trigger signal is generated after each ventilation cycle and used for gated OCT data acquisition, as described in Section 2.2. The measurement setup is illustrated in Figure 3. IVM and OCT are controlled by one PC running a LabVIEW user interface. A second PC controls the animal ventilator also using a custom-made LabVIEW program. The trigger signal is generated after each ventilation cycle and provided as 5 V TTL signal to a data acquisition device (USB 6009, National Instruments Germany GmbH, Munich, Germany) connected to the imaging PC, where it is used for continuous OCT data acquisition.
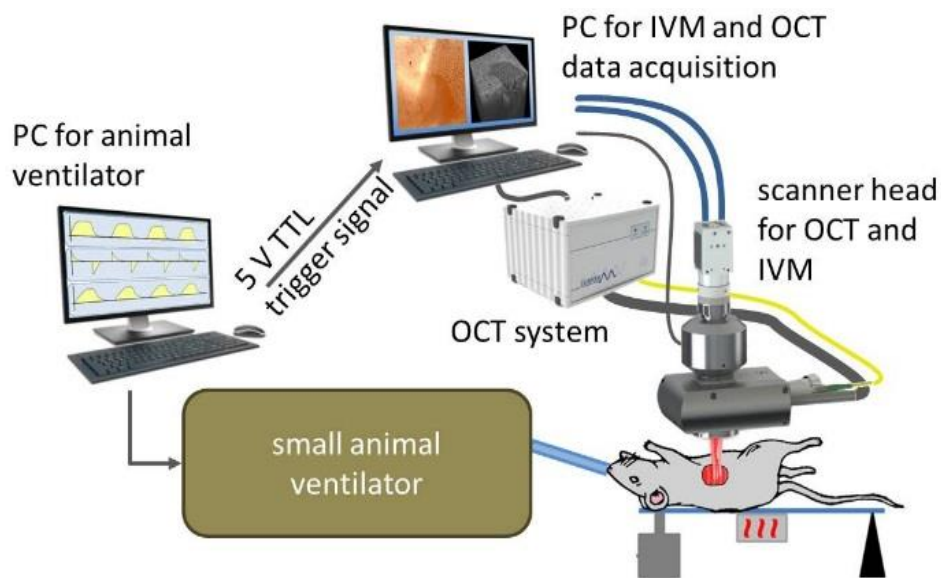

Figure 3. Measurement setup for investigating lung tissue dynamics. The animal is anesthetized and connected to the ventilator. Optical access to alveolar structures for OCT and IVM is achieved by resecting a thoracic window without harming the pleura visceralis in order to keep the physiological thoracic pressure conditions intact. The 5 V trigger signal generated from the ventilator is acquired by the imaging PC using an USB data acquisition board. The IVM image sequence is measured immediately before starting OCT data acquisition.

3. Results

The data acquisition during uninterrupted artificial ventilation with OCT and IVM was tested prior to the animal experiments. A periodic pattern from a function generator mimicking the movement of the pleura up to 1.5 Hz was applied to a loudspeaker with a structured target (data not shown). This enabled us to verify the functionality of the surface-tracking algorithm for IVM and the continuous OCT scanning mode with post-processing rearrangement of the acquired images.

Figure 4 shows exemplary measurement data during in vivo experiments. A collection of the measurement data for IVM and OCT is provided as a supplemental video file online (Video S1: 4D imaging of alveolar dynamics in ventilated rats). OCT and IVM images at four representative time points (during inspiration, at max. inspiration, during expiration and at max. expiration) were chosen to better illustrate the different positions and structures of the alveolar tissue. The pressure-time curve at the top of Figure 4 is a schematic of the used pressure-controlled ventilation mode during experiments performed with a frequency of 60 breaths per minute (f = 1 Hz) from 2 mbar (positive end-expiratory pressure) to 11 mbar (end-inspiratory pressure) with an inspiration-to-expiration ratio (I:E) of 1:1.
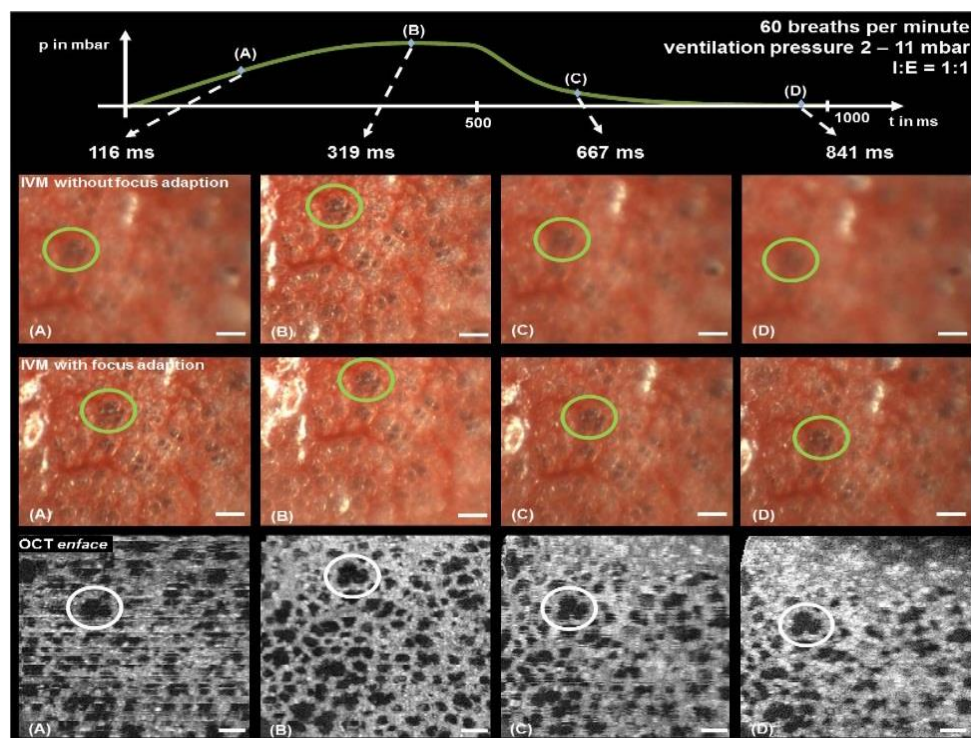
Figure 4. Visualization of lung tissue dynamics during artificial ventilation with OCT and IVM. Pressure-controlled ventilation was performed from 2–11 mbar at a frequency of 1 Hz and an inspiration-to-expiration ratio (I:E) of 1:1 showing a pressure-time course illustrated in the upper diagram. The advantage of the tunable liquid focus lens for IVM can be seen by comparing first and second rows. Most of the tissue movement cannot be imaged properly without focus adaption, so structural information was lost. By using the focus lens, the lung surface can be kept in focal plane over the whole ventilation cycle. The last row shows OCT enface images beneath the pleura calculated from the 3D image stacks. Image reconstruction works well after continuous OCT data acquisition especially in plateau phases (B and D). Small misalignments occur during phases of fast tissue movement (high slope of the pressure curve). One example of corresponding alveolar structures in both imaging techniques (OCT and IVM) is marked by the green and white circles. Scale bar is 150 μm.

It becomes clearly visible that the use of the tunable focus lens is essential to keeping the lung surface in focal plane for IVM over the whole ventilation cycle (compare to first row in Figure 4 "IVM without focus adaption"). Without tracking the lung surface, just a part of the video sequence (in this example at end-inspiratory plateau) is sharp enough to distinguish tissue structures and alveolar boarders. Compared to the second row of Figure 4, one can see the advantages of the electrically tunable focus lens for visualization of the tissue movement in axial direction over the whole ventilation cycle.

The last row of Figure 4 shows the corresponding OCT data stacks after rearrangement of the measured cross sections during uninterrupted artificial ventilation. OCT images show the average tissue movement during one ventilation cycle as enface view calculated from the 3D OCT stacks 25 μm beneath the pleura visceralis. Thereby, the alveoli become visible and the tissue structure can be compared to the IVM images (indicated by the green circle). During phases of high tissue movement in inspiration and expiration, image reconstruction is affected by disturbances as a result of jitter, as the B-scan was not synchronized to the ventilation or of the long overall measurement duration of 5.3 min (34 3D stacks with 320 × 320 × 512 pixels). Therefore, tissue movement is not exactly identical in each ventilation cycle, resulting in slight differences of the tissue structures within the OCT cross sections. This problem was mostly fixed by alignment of the pleura position during post-processing using open

source software FIJI [8]. With standard measurement parameters, the imaged area is 1.3×1.3 mm^2 and the pressure step resolution of adjacent 3D stacks is 0.53 mbar (9 mbar/17 stacks half and half for inspiration and expiration).

The advantage of OCT consists in the acquisition of real 3D image data, which provides more accurate information about structure and structural changes during ventilation than 2D images can. As an example, it is not completely clear from 2D IVM images whether all alveoli shrink during expiration or whether some of them move deeper into the tissue and therefore disappear from the image plane. This can be verified with 3D OCT data. For future experiments, the 3D volume of alveoli in the different phases of the ventilation cycle will be measured. In this experiment, the analysis of the area changes of the alveolar structures during ventilation was performed manually at five exemplary alveoli from OCT enface images, due to the large amount of image data and to the fact that no automatic algorithm for structure segmentation was yet available. All enface images were taken at the same position, 25 μm beneath the pleura, to assure comparability of the measured area. The segmentation was done manually in FIJI for five alveoli (marked by the numbers in the first image of Figure 5). Cross sections of Alveolus 1 (marked with the green dashed line) were taken to verify the findings from the enface segmentation regarding the area changes and the pressure-area loops (diagram of Figure 5). To illustrate these changes during ventilation, all measured alveolar areas were normalized to the area at end-expiratory pressure of 2 mbar. Therefore, all calculated pressure-area loops start at 1 (axis of ordinate) and 2 mbar (axis of abscissae). The measured changes from expiration to inspiration are within the range of 15%–25%, which is in good agreement to the results of other studies [9,10].
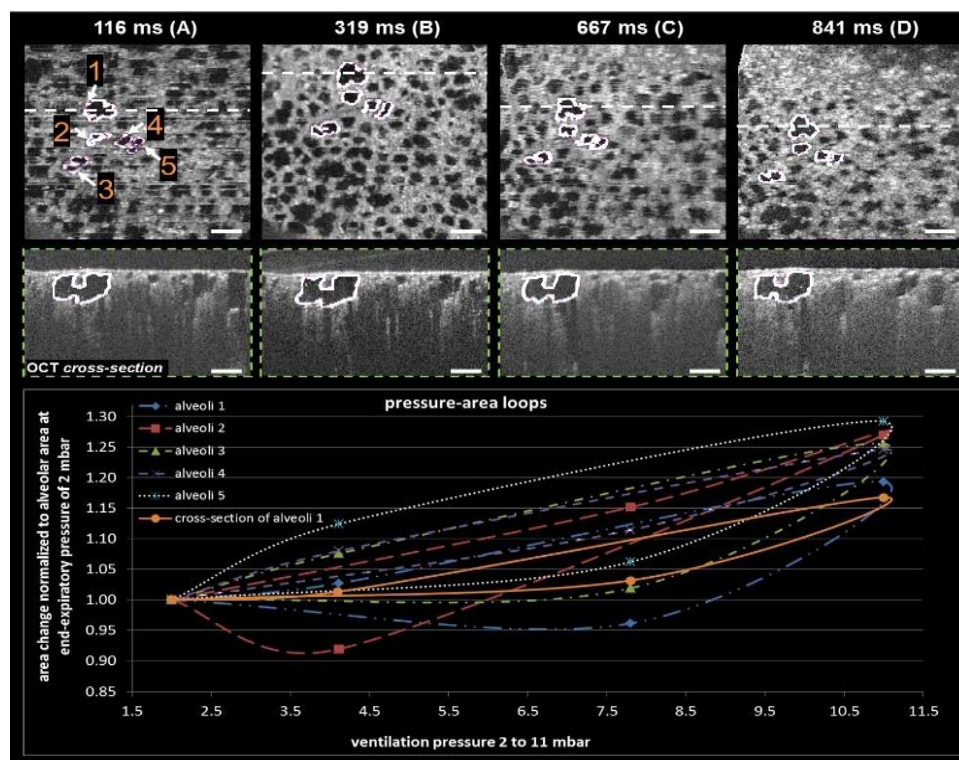

Figure 5. Segmentation of alveolar structures from OCT images and visualization of the pressure-area curves. First row shows OCT enface images 25 μm beneath the pleura and the five alveolar structures chosen for area measurement over the ventilation cycle. To verify these measurements, the cross-sectional view (cross sections taken along the dashed green line) was also taken and the area was measured, too. The pressure-area loops were plotted by normalizing the areas to the initial area at end-expiratory pressure of 2 mbar. The diagram shows the same course for all measurements with a small gap between inspiratory and expiratory area change. Scale bar is 150 μm.

4. Discussion

Investigating dynamic processes with high spatial and temporal resolution is a challenging task. Therefore, suitable imaging techniques and data acquisition protocols are necessary. We showed that OCT and intravital microscopy are promising tools for matching the effort of appropriated imaging techniques for the visualization of lung tissue movement during uninterrupted artificial ventilation in rats. A high-speed video camera and an electrically tunable focus lens controlled by the depth information obtained from fast scanning OCT cross sections were used to keep the lung surface in the focal plane during axial movement. This, allowed acquisition of video sequences over the whole ventilation cycle. The use of an external trigger signal from the animal ventilator in combination with a continuous OCT data acquisition mode enabled to employ a conventional OCT system (line scan rate 12 kHz) for the investigation of fast dynamic processes in vivo without the need of specialized high-speed OCT systems. Some limitations still remain beside these advantages. The continuous scanning mode enables the visualization of tissue movement over one ventilation cycle by combining images that were measured over several cycles. While this scheme works well during plateau phases (end of inspiration, end of expiration), jitter and other disturbances (from the tissue response on artificial ventilation) arising during phases of fast tissue movement result in small misalignments during the reconstruction of each individual 3D stack. This can be seen during the fast tissue movements in inspiration and expiration. Further work will deal with these disturbances on the one hand by improving the handshaking between the animal ventilator and the OCT system and on the other hand by developing a post-processing algorithm for the automatic alignment of adjacent cross sections. Especially, the first point has a major impact on the jitter of the OCT data shown in this paper. As OCT data capture and ventilation are not synchronized, images with a shift of up to one frame period (29 ms) are combined to one volume. This problem will be avoided in future measurements by implementing bidirectional handshaking. For this purpose, the OCT system will also give a trigger signal to the ventilator when an image is still acquired, and the ventilator will wait up to 29 ms before triggering the OCT system. This additional time of 29 ms will influence the breathing rate only marginally, but will help prevent the jitter in the rearranged 3D OCT stacks. Furthermore, we will combine other imaging techniques such as confocal fluorescence microscopy to gather functional information of elastic fibers surrounding the alveoli during artificial uninterrupted ventilation. Finally, new segmentation algorithms will be implemented to handle the mass of image data, and automatically extract alveolar volume changes and tissue characteristics from the 3D OCT stacks.

5. Conclusions

This feasibility study shows that emerging imaging techniques such as OCT in combination with IVM are promising tools for gaining new insights into alveolar dynamics during artificial ventilation in animal experiments. Such measurements can provide necessary information about tissue behavior and promote an understanding of micromechanics that can lead to the development of more protective ventilation strategies.

Author Contributions: All authors contributed equally to the paper. Christian Schnabel and Edmund Koch developed the OCT data acquisition and the small animal ventilator. Christian Schnabel performed all the measurements and segmentations and wrote the paper. Maria Gaertner prepared the animal experiments and developed a method of visualizing the 4D OCT data.

Conflicts of Interest: The authors declare no conflict of interest. The funding sponsors had no role in the design of the study; in the collection, analyses, or interpretation of data; in the writing of the manuscript; or in the decision to publish the results.

References

1. WHO. *World Health Statistics*; WHO: Geneva, Switzerland, 2016.
2. Petrucci, N.; Feo, C.D. Lung protective ventilation strategy for the acute respiratory distress syndrome. *Cochrane Database Syst. Rev.* **2013**, *2*.
3. Serpa Neto, A.S.; Cardoso, S.O.; Manetta, J.A.; Pereira, V.G.M.; Espósito, D.C.; Pasqualucci, M.O.; Damasceno, M.C.T.; Schultz, M.J. Association between Use of Lung-Protective Ventilation with Lower Tidal Volumes and Clinical Outcomes among Patients Without Acute Respiratory Distress Syndrome a Meta-analysis. *JAMA* **2012**, *308*, 1651–1659. [CrossRef] [PubMed]
4. Unglert, I.C.; Namati, E.; Warger, C.W., II; Liu, L.; Yoo, H.; Kang, D.; Bouma, E.B.; Tearney, J.B. Evaluation of optical reflectance techniques for imaging of alveolar structure. *JBO* **2012**, *17*, 071303. [CrossRef] [PubMed]
5. Schnabel, C.; Gaertner, M.; Kirsten, L.; Meissner, S.; Koch, E. Total liquid ventilation: A new approach to improve 3D OCT image quality of alveolar structures in lung tissue. *Opt. Express* **2013**, *21*, 31782–31788. [CrossRef] [PubMed]
6. Kirsten, L.; Gaertner, M.; Schnabel, C.; Meissner, S.; Koch, E. Four-dimensional imaging of murine subpleural alveoli using high-speed optical coherence tomography. *J. Biophotonics* **2013**, *6*, 148–152. [CrossRef] [PubMed]
7. Meissner, S.; Knels, L.; Krueger, A.; Koch, T.; Koch, E. Simultaneous three-dimensional optical coherence tomography and intravital microscopy for imaging subpleural pulmonary alveoli in isolated rabbit lungs. *JBO* **2009**, *14*, 051020. [CrossRef] [PubMed]
8. Schindelin, J.; Arganda-Carreras, I.; Frise, E.; Kaynig, V.; Longair, M.; Pietzsch, T.; Preibisch, S.; Rueden, C.; Saalfeld, S.; Schmid, B.; et al. Fiji: An open-source platform for biological-image analysis. *Nat. Methods* **2012**, *9*, 676–682. [CrossRef] [PubMed]
9. Mertens, M.; Tabuchi, A.; Meissner, S.; Krueger, A.; Schirrmann, K. Alveolar dynamics in acute lung injury: Heterogeneous distension rather than cyclic opening and collapse. *Crit. Care Med.* **2009**, *37*, 2604–2611. [CrossRef] [PubMed]
10. Gaertner, M.; Cimalla, P.; Meissner, S.; Kuebler, W.M.; Koch, E. 3D simultaneous optical coherence tomography and confocal fluorescence microscopy for investigation of lung tissue. *J. Biomed. Opt.* **2012**, *17*, 071310. [CrossRef] [PubMed]